Flaw Effects and Flaw Reorientation on Spent Fuel Rod Performance, a Simulation with Finite Element Analysis

David T. Tang, Antonio Rigato, Robert Einziger[1]
U.S. Nuclear Regulatory Commission (NRC)
Washington, DC 20555-0001
David.Tang@nrc.gov

ABSTRACT: While fuel cladding failures have decreased significantly over the years, fuel cladding can still develop defects in the form of cracks, blisters, and circumferential hydride precipitates when irradiated. After drying for storage, circumferential precipitates may reorient as radial hydrides. This study examines if these hydrides could potentially influence the bending performance of the rod. Using a hollow, simply supported fuel tube to simulate the limiting behavior of a spent fuel rod deprived of the flexural rigidity contribution of the pellets, effects of the hydrides presence and orientation on the fuel rod bending structural performance are assessed. Within the confines of the finite element analyses (FEAs) of a flawed bare fuel tube, the bending strength of the hollow tube is shown not to be significantly compromised by the presence of the modeled circumferential and radial hydrides.

INTRODUCTION

In the criticality, containment/confinement, thermal, and shielding safety evaluations, the U.S. Nuclear Regulatory Commission (NRC) staff seeks reasonable assurance that spent fuel rods will maintain their analyzed configurations after a spent fuel storage or transportation cask drop accident. A FEA is commonly performed using the cladding's Young's modulus, yield strength, and ductility commensurate with the level of irradiation, to calculate permanent deformations, if any, as an estimate of fuel rod assembly geometric reconfiguration. For low burn-up PWR fuel, cask vendors have relied on ductile cladding material properties to demonstrate acceptable fuel rod geometric performance, for certain cask handling accidents. Since a similar set of cladding material properties for high burn-up fuel suitable for FEA calculation are generally hard to obtain for the range of cladding materials in use, cask vendors have had only limited cases where analysis can be used to qualify high burn-up fuel for either storage or transportation cask drop accidents. It is important to note that recent tests have shown that high burnup fuel cladding is still quite ductile (1).

In this paper, defects in the fuel cladding due to handling, manufacturing, or use, are simulated as thin, slit-like flaws, and are examined for their effects on the bending stress performance of a fuel tube with two separate flaw configurations. Using the ρ-□-z cylindrical coordinate system, "circumferential" flaws, shown schematically in Figure 1-a, are seen to reside in the □-z plane. If the same flaws were to rotate about the long axis of the tube (z-axis), the resulting configuration would be the "radial" flaws shown in Figure 1-b, which lie in the ρ-z plane.

Using strength of materials structural analysis approach in the FEA simulation below, the effect

[1] Since writing this paper, Dr. Einziger has moved on to become Senior Professional Staff at the US Nuclear Waste Technical Review Board.

of the presence of a pair of similar flaws on the stress performance of a bare fuel tube is investigated. This is done by first examining the disruption of the fuel tube stress field due to the presence of a flaw pair for both the radial and circumferential orientation. Next, the extent to which the disrupted stress field in the cladding recovers is examined as a function of the distance between two similar flaws.

FINITE ELEMENT ANALYSIS SIMULATION

Model Description. The FEA simulation is configured to examine the bending structural performance of a bare fuel tube subject to lateral inertia loading. Figure 2-a shows schematically the FEA model consisting of a simply supported 5 inch (127 mm) long hollow fuel tube with wall thickness of 0.025 inches (0.635 mm) and outer diameter of 0.382 inches (9.70 mm). Consistent with current fuel rod buckling analysis practice, the stiffness the fuel pellets add to the flexural rigidity of the fuel rod is conservatively neglected to simulate the limiting fuel rod behavior (2). Figure 2-b and 2-c depict the circumferential and radial flaw pairs considered where each flaw measures 0.03 inches (0.762 mm) long by 0.015 inches (0.381 mm) wide and 0.005 inches (0.127 mm) thick at a 6:3:1 aspect ratio. The flaws themselves can be thought of as one large flaw or several flaws clustered together. The flaw size is selected primarily for ease of FEA modeling with limited computing resource. ANSYS Mechanical APDL V14.5.7 is used to generate the FEA input files using the default auto mesh generator. Taking advantage of the symmetry plane at the mid-span, the tube is modeled with up to 35,000 20-node ANSYS SOLID 186 elements with additional element options utilized for maximum accuracy. Because only the degree of stress field variation is of interest and localized plasticity at stress riser locations is not a concern, an elastic analysis is performed of the tube for a 1-g gravitational load, using a Young's modulus of 11.0×10^6 psi (75.7 GPa) and a Poisson's ratio of 0.404 (3). For the undamaged tube with no cladding flaws, the maximum stress (pure bending and no shear) at the mid-span extreme fiber on the compressive side of the tube surface is calculated to be 8.84 psi (0.0609 MPa).

At the mid-span tube circumference, a stress field disruption is assumed to have occurred in the cladding if the stress at a distance of one flaw thickness of 0.005" (0.127 mm) away from the flaw edge is shown about 10% above the calculated "nominal" stress at that location for the undamaged cladding scenario. Along the tube axial direction, stress field recovery is assumed to have occurred between two flaws if the stresses half way between them are shown to be within 10% of the nominal stress that exists at that location for an undamaged tube. As depicted in Figure 2-b and 2-c, one flaw of the flaw pair is always located at mid-span, while the second is a distance away that is a multiple of the width dimension (0.015") "W", of the flaw. The dimension W is used since it represents the larger of the two dimensions, W and T (thickness), characterizing the area that causes stress disruption, and lends itself well to the examination of stresses using St. Venant's principle. Results detailed below focus on stresses orientated in the axial direction (z).

Stress Field Disruption. Figures 3-a and 3-b show the prospective close-ups of the "half" circumferential and radial flaws, respectively, at the mid-span symmetry plane. Figures 4-a and 4-b display fringe plots for stress field disruptions around the mid-span flaws for the two flaw pairs analyzed. The "square" tip portion of the flaw sees a maximum stress of -18.7 psi (-0.129 MPa) for the circumferential flaw, while the flaw in the radial direction generates a maximum value of 14.7 psi (-0.101 MPa) as compared to the unflawed cladding value of -8.84 psi (-0.061 MPa). Along the mid-span tube circumference and beyond about one flaw thickness distance of 0.005" (0.127 mm), stresses of -9.78 psi (-0.067 MPa) and -9.83 psi (-0.068 MPa) are calculated for the circumferential and radial flaws, respectively. For both circumferential and radial flaws, stresses are seen to rise close to 10% of the nominal stress of -8.84 psi (-0.0609 MPa) then quickly fall below it at a circumference distance of about one flaw thickness. This lack of stress field disruption is not unexpected since, except at the very "tip" of the flaw, the development of the bending stress normal to the tube cross-sectional cut is barely hindered by the presence of these two flaw types.

The results presented above are based on an elastic analysis with only two flaws. With a sufficiently large lateral loading, the elastic stress analyses indicates that the flaw tips will be first to experience material yielding. However, because of stress redistribution, yielding at flaw tips is expected to be isolated and not to grow into to the surrounding undamaged material.

Stress Field Recovery. While specific stress values are of significance for describing a general trend of stress field disruption, observation on how the disrupted stress field may recovery could be of great interest to researchers. Figures 5 and 6 display stress fringe plots for the circumferential and radial flaw cases, respectively. Along the tube axial direction, the distance required between a radial flaw pair and a circumferential flaw pair for the stress field to recover is recorded. Specifically, a "characteristic" distance of only 4W is required for both radial and circumferential flaws. As to the individual stress magnitude, within the small area with a length defined by half the characteristic distance and a width not more than half the characteristic distance, stresses associated with the circumferential and radial flaws are all below the nominal stress value of the undamaged tube. The distance away from the flaw that St. Venant's principle would expect a minimal change in stress distribution is at about 2W away. At 2W away, stress values are within 5% of the expected stress value for the circumferential flaw pair, and 3% for the radial flaw pair.

Visualization of Stress Field Disruption and Recovery. From a macroscopic structural analysis perspective, the evaluation above shows that the reorientation of flaws only makes a minimal difference to the fuel tube bending capability in only a very limited area. This perspective of stress disruption and recovery can also be described from a streamline analogy using uniform fluid flow in a pipe, where the flow is partially obstructed by a thin plate, which is analogous to the flaw in this investigation. In the region of the fuel cladding examined, the "flow" is dominated by bending stresses which act perpendicular to the tube cross section. The flaws that disrupt these stresses the most are those that "obstruct" more of the tube's cross section. Both radial and circumferential flaws constrict flow in nearly the same way because they block the same amount of area.

Implication on High Burn-up Fuel Bending Performance

While the previous evaluation is for a generic flaw, post-irradiation characterization of spent fuel has revealed the most predominant flaw to be precipitated circumferential hydrides caused by the absorption of a fraction of the hydrogen produced by the oxidation of the exterior cladding surface. In high burnup fuel there is a sufficient amount of hydrides, and high enough cladding hoop stress that, under the temperatures associated with drying, some of these circumferential hydrides may reorient to the radial direction (see Figure 7).

Effects of these hydrides on the performance of the fuel rods have for some time been a point of conjecture in the nuclear industry. For spent fuel subject to either a cask side-drop or an end-drop accident scenarios, due to the relative alignment of the dominant stress components with respect to the hydride orientation in the cladding and assuming that there is sufficient distance circumferentially and axially between the flaws of sound cladding material, the FEA simulation suggests that presence of circumferential and radial hydrides should not have much effect on the fuel rod bending performance.

As for irradiated fuel subject to cask vibration under normal conditions of transport, the FEA results also suggest that fatigue tests with radial hydrides in the cladding should not deviate from the test results for the case with circumferential hydrides. In the vibratory testing recently completed at the Oak Ridge National Laboratory for high burnup (~65 GWd/MTU) PWR rod segments, fatigue S-N curves are reported for the case of circumferential hydrides (1). Supplemental testing is under way for rodlets that have had radial hydrides introduced into them.

Based on the size and distribution of the radial hydrides observed from existing metallography, two potential outcomes may be realized when the FEA results are compared to test results for the case of radial hydrides:

- Experimentally there is little difference in fatigue behavior between the two sets of samples, which is the expected result extrapolated from the FEA simulation.

- There is an appreciable difference in the fatigue behavior between the two sets of samples suggesting that intricacies unique to radial hydrides are significantly different than those of the circumferential hydride which has not been sufficiently captured in this FEA, or, an unknown rod failure mechanism yet to be identified is affecting the results.

CONCLUSION

This investigation presents a finite element analysis simulation of cladding flaws with two orientations (circumferential and radial) characterized as material discontinuities. Using a hollow, simply supported fuel tube to simulate the bounding performance of a spent fuel rod, effects of the presence of cladding flaws and their reorientation on the fuel rod bending strength are assessed. With a limited number of elastic sensitivity analyses, the simulation results

suggest that fuel cladding should not be greatly affected by flaw reorientation, nor by their presence as modeled if the cladding material adjacent to the flaws is able to adequately support the redistribution of localized stress concentrations. Since hydrides are known only to form in the respective □-z and ρ-z planes FEA simulation suggests that hydride presence and reorientation will have little impact on the fuel rod bending performance in a cask drop accident or the fatigue strength when subject to cyclic bending vibration encountered during normal conditions of transport.

ACKNOWLEDGMENTS

The authors are indebted to Dr. Gordon Bjorkman for many of his valuable comments during the development of the paper.

REFERENCES

1. J-A Wang and H. Wang, “Mechanical Fatigue Tests of High-Burnup Fuel for Transportation Application,” NUREG/CR-7198, ORNL/TM-2014/214, Oakridge National Laboratory, Oak Ridge, TN, April 2015.

2. H. E. Adkins, Jr., B. J. Koeppel, and D. T. Tang, “Spent Nuclear Fuel Structural Response When Subject to an End Impact Accident,” American Society of Mechanical Engineers, Pressure Vessels & Piping Division, vol. 483, pp. 207-214, American Society of Mechanical Engineers, New York, NY, 2004.

3. C. L. Whitmarsh, “Review of Zircaloy-2 and Zircaloy-4 Properties Relevant to N.S. Savannah Reactor Design,” Oak Ridge National Laboratory, Contract No. W-7405-eng-26.

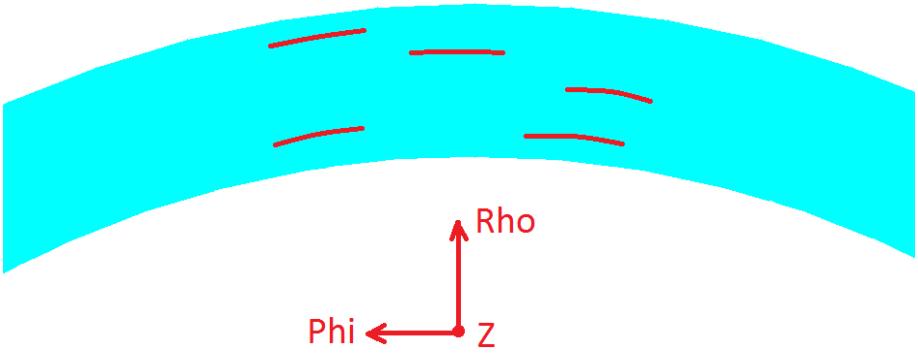

Figure 1-a Sample Circumferential Flaws (Phi Direction) in the □-z Plane

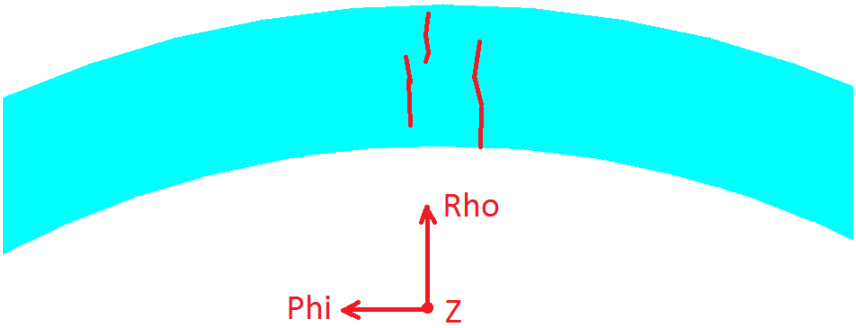

Figure 1-b Sample Radial Flaws (Rho Direction) in the ρ-z Plane

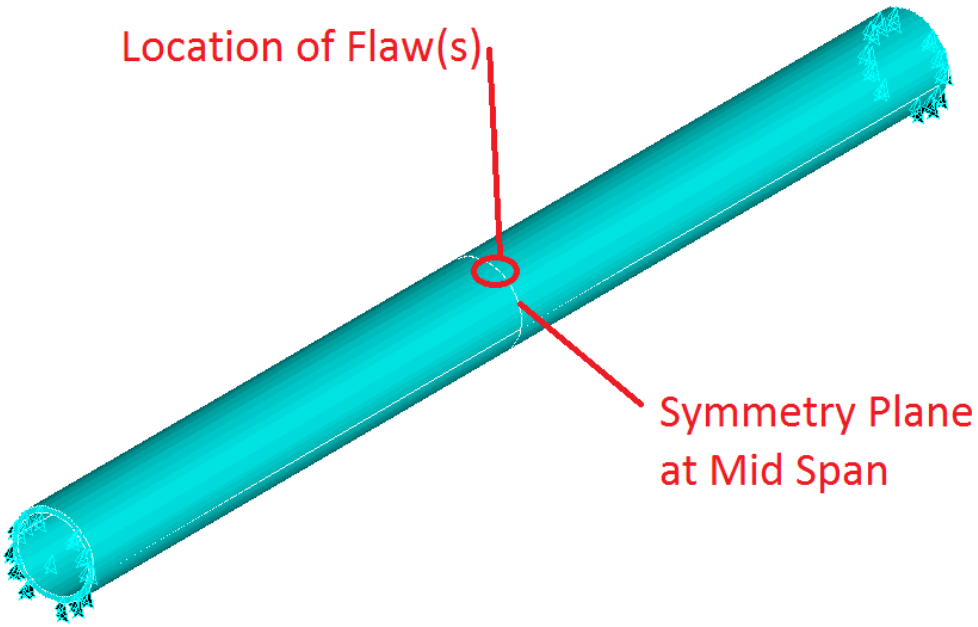

Figure 2-a Schematic of a Simply Supported Tube, General Flaw Location Relative to Symmetry Plane at Mid-Span.

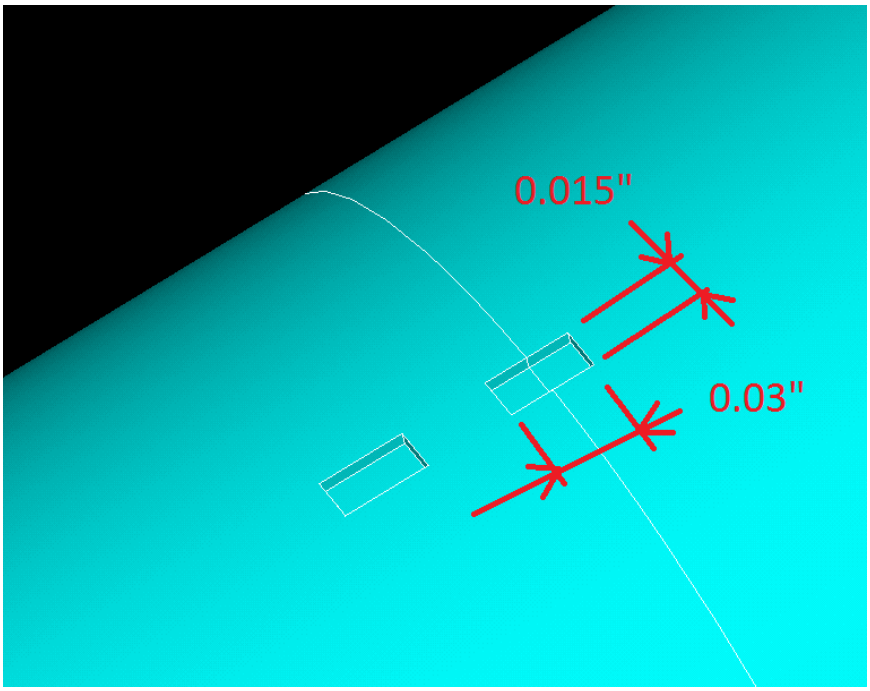

Figure 2-b Close-up of Circumferential Flaw Pair.

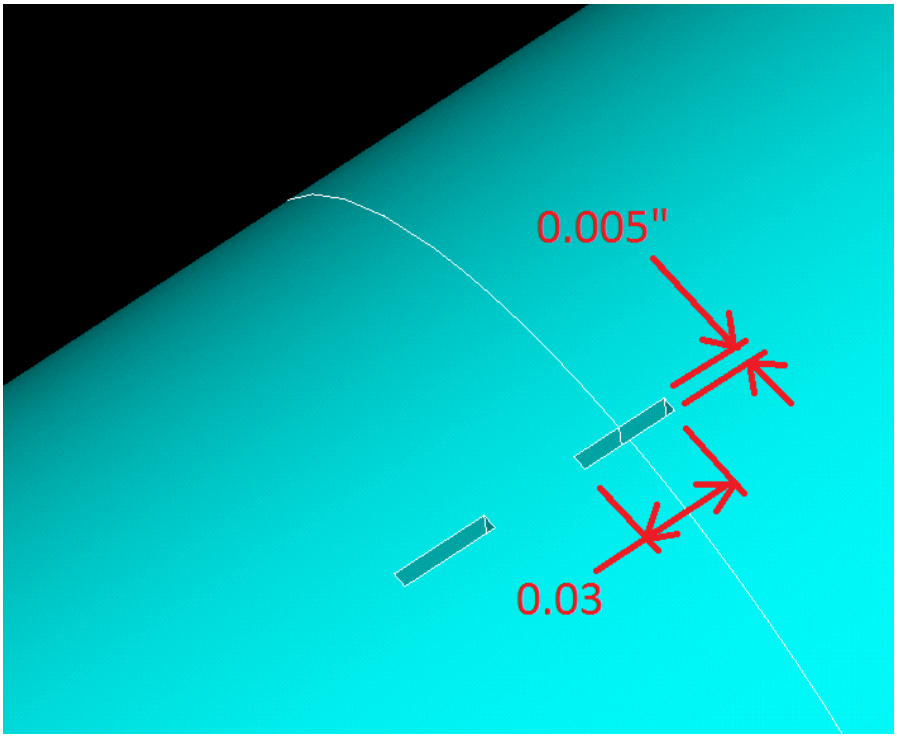

Figure 2-c Close-up of Radial Flaw Pair.

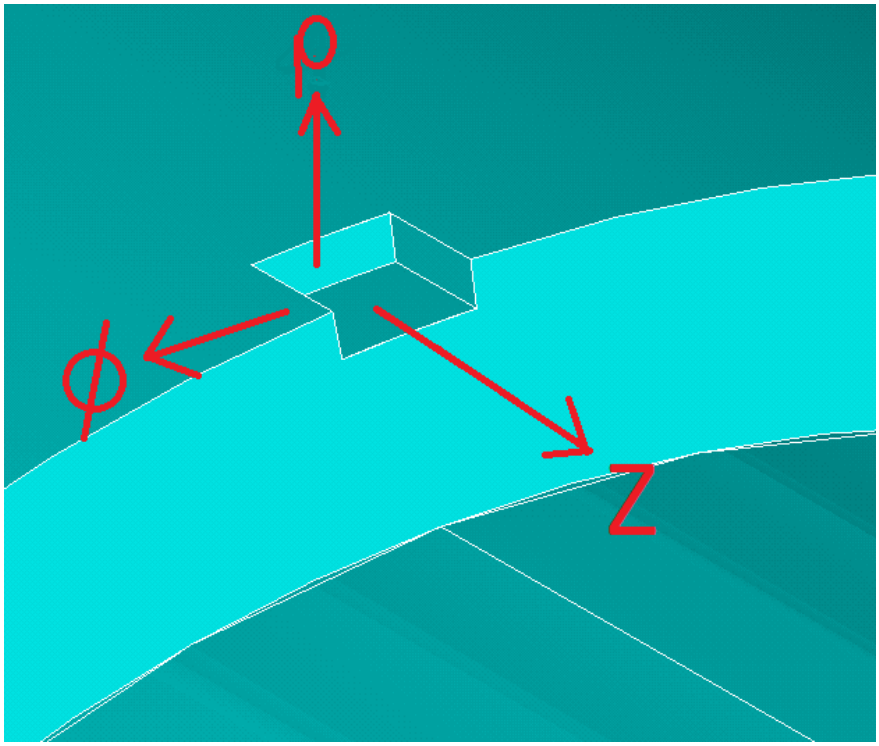

Figure 3-a Circumferential Flaw at the Surface, Half Flaw Length into Axial Direction at Symmetry Plane

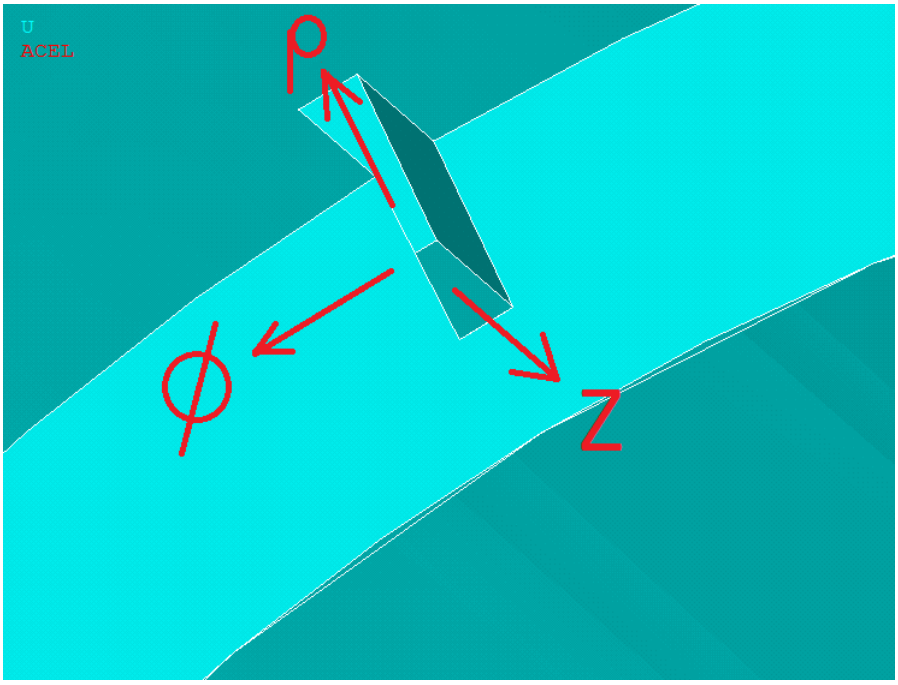

Figure 3-b Radial Flaw at the Surface, Half Flaw Length into Axial Direction at Symmetry Plane

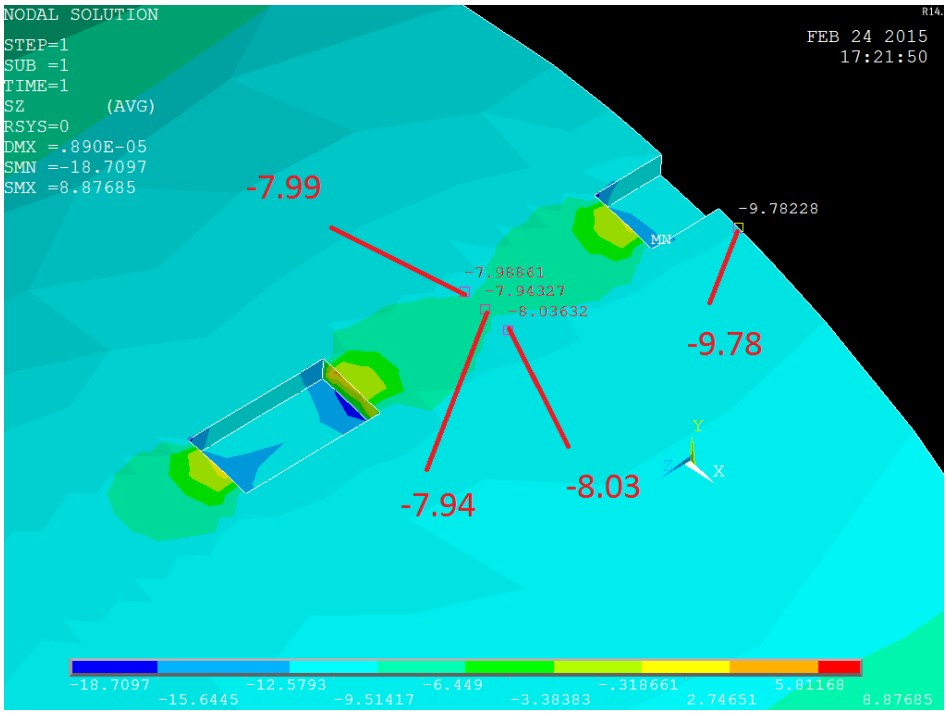

Figure 4-a Stress (psi) in the Axial Direction (z) for a Circumferential Flaw Pair, 4W (0.06") between Flaws

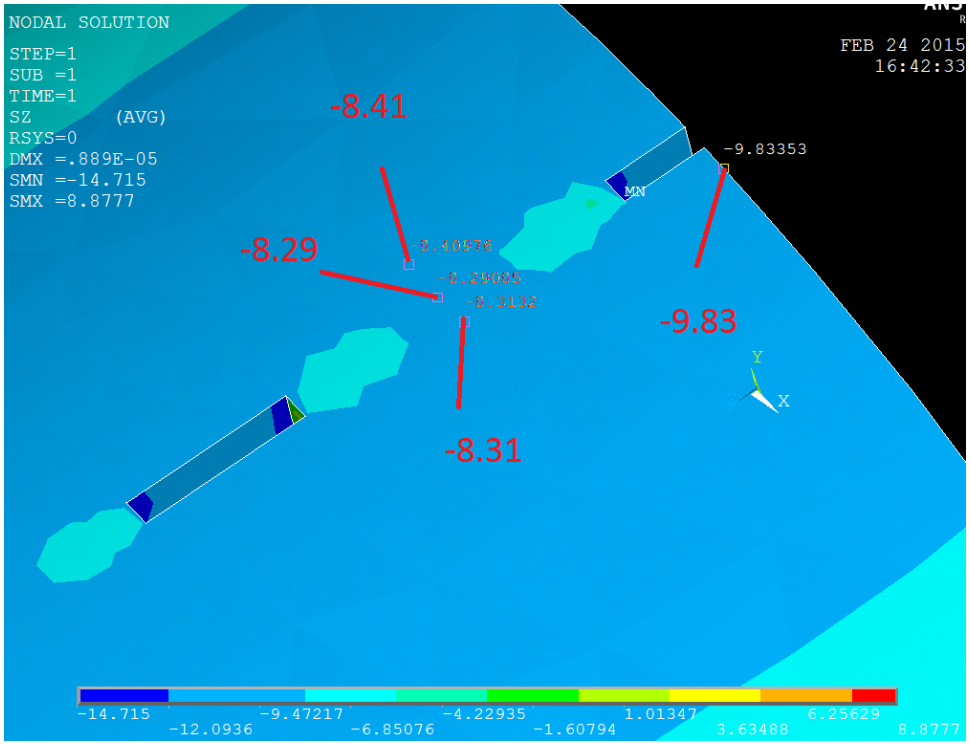

Figure 4-b Stress (psi) in the Axial Direction (z) for a Radial Flaw Pair, 4W (0.06") between Flaws

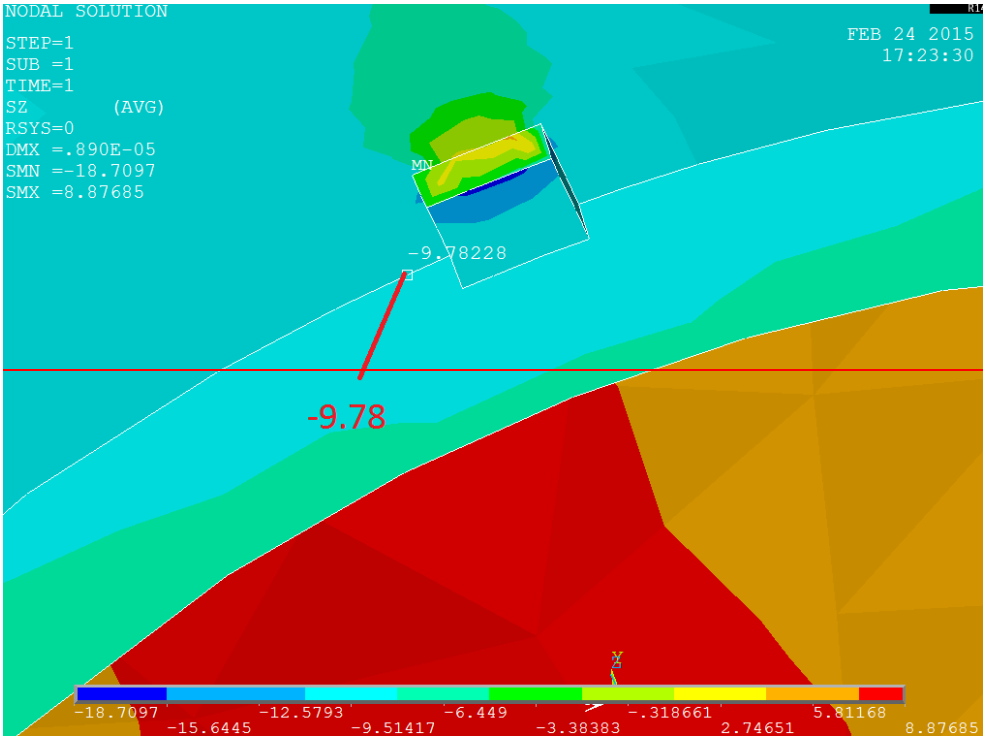

Figure 5 Stress (psi) in the Axial Direction (z) for a Circumferential Flaw, Mid-Span Circumference

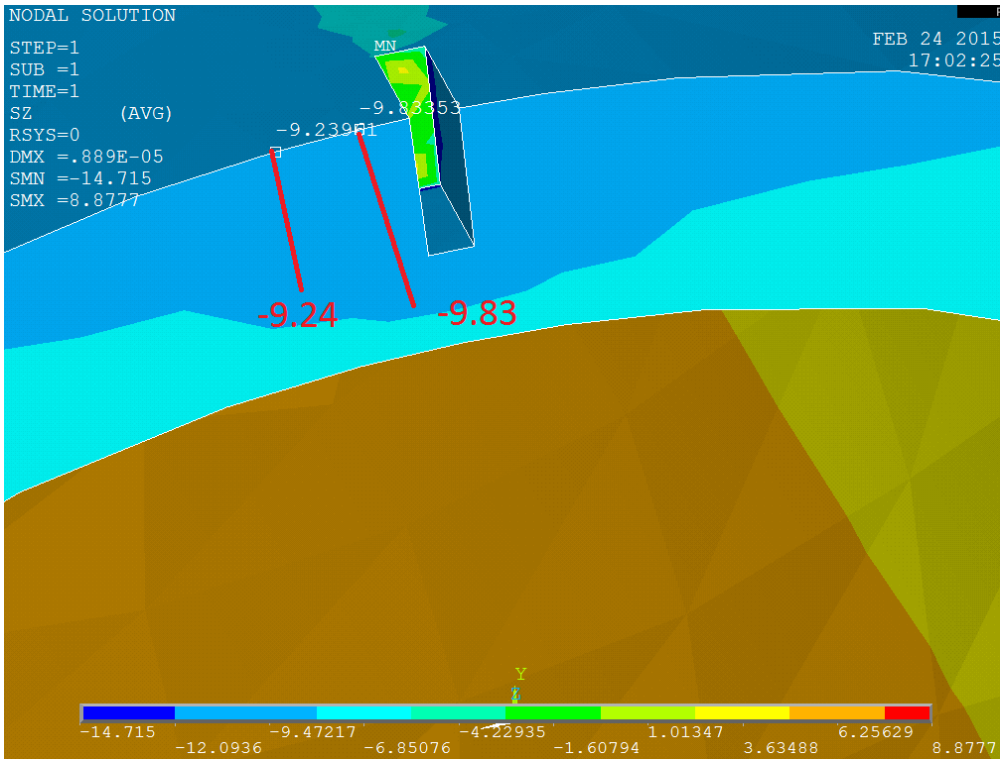

Figure 6 Stress (psi) in the Axial Direction (z) for a Radial Flaw, Mid-Span Circumference

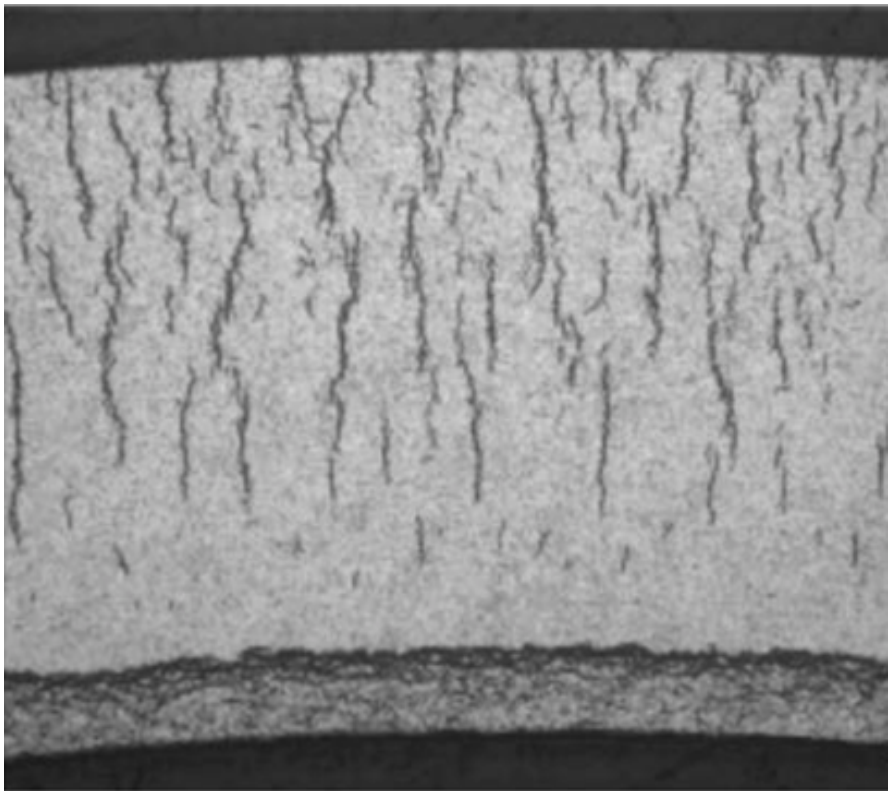

Figure 7 Observed Cladding Radial Hydrides in a PWR Fuel Rod